J Therm Anal Calorim (2012) 108:1261–1272
DOI 10.1007/s10973-011-1710-7

Thermal and structural properties of surfactant–picrate compounds

Effect of the alkyl chain number on the same ammonium head group

Tea Mihelj · Zoran Štefanić · Vlasta Tomašić

Received: 11 April 2011 / Accepted: 26 May 2011 / Published online: 17 June 2011

Abstract The novel surfactant–picrate compounds were synthesized and characterized by thermal and XRD analysis. The synthesis, based on the electrostatic interactions of components in polar solvents, was carried out using picric acid and cationic surfactants (dodecyltrimethylammonium, didodecyldimethylammonium, and tridodecylmethylammonium halide). The idea was to investigate the dependence of physico-chemical properties and thermal transitions of picrate–surfactant compounds with raising number of dodecyl chains sited on the same ammoniumm head group. The equimolar mixed aqueous solutions are characterized as lyotropic, strongly promoted by picrate anion. The main crystal structure feature of investigated picrates is layered structure with stacked aromatic rings of one picrate molecule on the top of the other one via strong $\pi \ldots \pi$ interactions and connection to the alkylammonium molecules with their nitro groups by C–H…O hydrogen bonds. Surfactant–picrate bilayer-like structures are interrupted with layers of polar heads and picrate counterions and the observed width of such a bilayers are functions of more complex structural behaviors which ensures alternation in space of equal numbers of positive and negative charges. Although some of the surfactants used posses thermotropic porperties, like examined tridodecylmethylammonium chloride, no thermotropic mesomorphism is detected in solid state of investigated surfactant–picrate compounds. The thermodynamic parameters of solid–liquid thermal transitions depend linear on the number of dodecyl chains, and for double- and triple-tailed picrate compounds the marked temporal hysteresis of the melt crystallization is registered.

T. Mihelj · Z. Štefanić · V. Tomašić (✉)
Department of Physical Chemistry, Ruđer Bošković Institute, POB 180, 10002 Zagreb, Croatia
e-mail: vlasta.tomasic@irb.hr

Keywords Thermal analysis · Alkyl chain number · Cationic surfactant · Picrate · Crystal structure

Introduction

In this article, we report the preparation, physico-chemical properties, and characterization of series of chemical structures with the picrate unit and single-, double-, and tri-tailed alkylammonium cationic amphiphiles, with the same length of the attached alkyl chain.

Nowdays, there is a considerable interest in the general area of colloidal and organic solid-state chemistry, particularly in the understanding of factors which control the arrangement of molecules in a crystal lattice, where the influence of surfactants with different molecule structures is one of those factors. The picrate anion is chosen because of its property to form often nicely crystalline solids, and is generally useful for the separation, purification, and identification of many organic compounds. The picric acid forms stable ionic salts or charge transfer complexes with many aromatic hydrocarbons, alkalines, aliphatic or aromatic amines [1–4] as the most important functional groups in molecules of biological importance, including amino acids, nucleoside, proteins, vitamines, and alkaloids [5–7]. The most favorable interaction site is negatively charged phenolic oxygen due to ion–ion interaction, where the picrate coordinates as a monodentate ligand and the crystal structure consists of molecules of an anion and cation connected by hydrogen bonds [3, 4]. Possible simultaneous interactions with *o*-nitro and *p*-nitro oxygens may lead to the formation of multidentate anions [8]. Studies of the picrate interactions may be used for various scientific and commercial applications, from dye and explosive manufacturing to biological monitoring methods [1].

The appropriate combination of experimenal techniques in the investigation of the interactions of single- and multi-tailed cationic surfactants with oppositely charged picrate molecules should provide more valuable information about the nature of interactions of some anionic fragments with different cationic surfactants, and about the variety of product structures and their physico-chemical properties. Seldom some authors pointed out the neglected role of the ionic surfactant tails [9], mainly with identical headgroup but differing tail lengths [10, 11]. The solid to liquid crystal phase transition temperatures and enthalpies [11] and mesophase-isotropic transition temperatures [10] show a linear dependence with the chain length. This work is a continuation of our research effort focused on the interplay between molecular architecture, intermolecular interactions, order, and macroscopic properties, investigating the complex polymorphism, thermotropic mesomorphism, and supramolecular organization of catanionic surfactants [10].

Experimental

Materials

The picric acid i.e. 2,4,6-trinitrophenol (p.a., Merck), and the cationic surfactants: dodecyltrimethylammonium bromide (Fluka, >99.0% AT, critical micelle concentration, *cmc*/mmol $dm^{-3} = 17$ [12]), didodecyldimethylammonium bromide (Acros Organics, >99.0% AT; *cmc*/mmol $dm^{-3} = 0.05$ [13]; critical vesicle concentration, *cvc*/mmol $dm^{-3} = 0.014$ [14]), tridodecylmethylammonium chloride (Fluka, ≥97.0% AT, *cmc* unknown) and tetradodecylammonium bromide (Fluka, ≥99.0% AT, *cmc* unknown) were used without further purification for the preparation of solid salts.

Synthesis of surfactant picrates

Cationic surfactant picrates were prepared by mixing cationic surfactant halides and picric acid at equivalent conditions. All systems are prepared at the same final concentration of 0.005 mol dm^{-3} in heated aqueous solutions, thermostated at $T/K = 293 \pm 0.1$ and aged for a period t_A. The exceptions were tridodecylmethylammonium picrate prepared in acetone due to the solubility reason, and the attempts to prepare tetradodecylammonium picrate in ethanol, acetone, or toluene was unsuccessful. The microcrystalline compounds were precipitated as darker or brighter yellow needles. They were collected by filtration after 2 weeks of aging, washed with cold water to remove potentially coprecipitated electrolyte, recrystallized several times from ethanol and acetone, dried under vacuum for 24 h at room temperature, and stored protected from moisture and light before use. Isolation of the extremely small particles of the separated phase for the X-ray powder diffraction experiments was performed after 60 min of systems aging by 60 min centrifugation at 36,000 rpm (Beckman L2-65B ultracentrifuge with rotor 40). Single crystals were grown using slow evaporation solution growth technique in refrigerator.

Novel compounds are presented in Scheme 1 and marked as follows: dodecyltrimethylammonium picrate (refered as compound **1**), didodecyldimethylammonium (**2**), and tridodecylmethylammonium picrate (**3**). The purity of compounds was checked by elemental analysis. Anal. for $C_{21}H_{36}N_4O_7$ (**1**) found: C, 55.20; H, 7.96; N, 12.26%; requires C, 55.22; H, 7.95; N, 12.27%; for $C_{32}H_{58}N_4O_7$ (**2**) found: C, 62.90; H, 9.56; N, 9.16%; requires C, 62.92; H, 9.57; N, 9.17%; for $C_{43}H_{80}N_4O_7$ (**3**) found: C, 67.48; H, 10.56; N, 7.33%; requires C, 67.50; H, 10.54; N, 7.32%.

Measurements

The mean hydrodynamic diameter of vesicles formed short after preparation of compounds in aqueous solutions was measured using dynamic light scattering (DLS) by a Zetasizer Nano ZS (Malvern, UK) equipped with a 532 nm "green" laser. Detection occurred at 173° angle in glass cuvettes. A latex standard of uniform particle size of 20 nm was used to evaluate the accuracy of the measurements. Mean hydrodynamic diameter of vesicles, d (nm), was estimated using Debye–Einstein–Stokes equation $d = k_B T/(3\ \pi\ \eta\ D)$, where k_B represents the Boltzman constant, T is the absolute temperature (298 K), η is the viscosity of the dispersing medium, and D is the apparent diffusion coefficient.

The morphology and texture of samples were observed between slide and cover slip by a optical polarizing microscope Leica DM LS equipped with a Mettler FP 82 hot stage and a color video camera Sony model No. SSC-DC58AP. The average size of vesicles coexisting with precipitate was estimated from series of microphotographs.

Elemental analyses were performed on a Perkin-Elmer Analyser PE 2400 Series 2.

Thermogravimetric analysis, TGA, was performed from 293 to 600 K with a Mettler Toledo TA 4000 system.

Thermal properties were examined by differential scanning calorimetry, DSC, using Perkin-Elmer Pyris Diamond DSC calorimeter in N_2 atmosphere equipped with a model Perkin-Elmer 2P intra-cooler. Solid samples were placed in an aluminum hermetic pans, heated, and cooled (in some cases to 263 K) at the rate of 5 K min^{-1}. Temperature and enthalpy calibrations were performed using high purity standard (*n*-decane and indium). The transition temperatures, T, were reported as the maximum and minimum of their endothermic and exothermic peaks. The resulted transition enthalpy, ΔH (kJ mol^{-1}), was

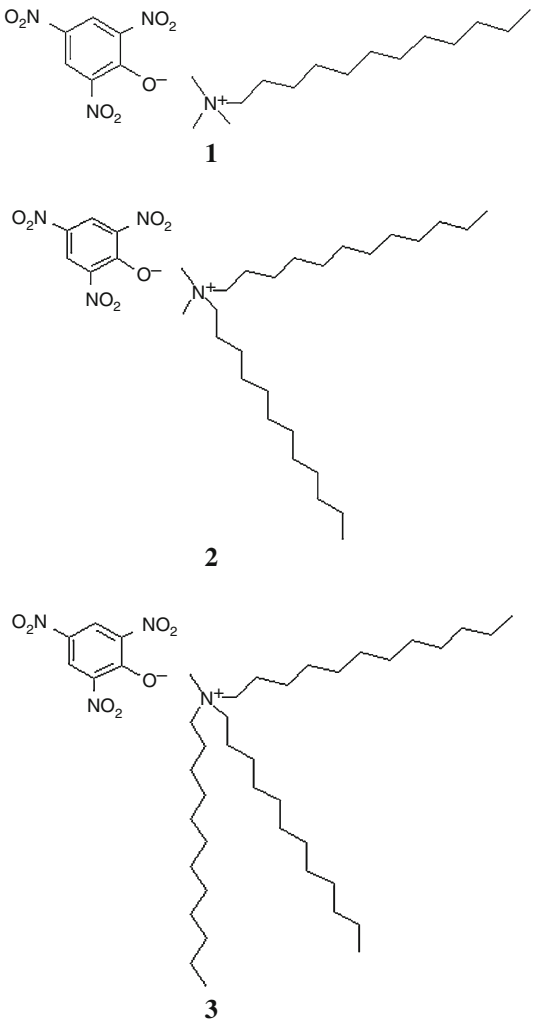

Scheme 1 The scheme of the investigated picrates: dodecyltrimethylammonium picrate (**1**), didodecyldimethylammonium picrate (**2**), and tridodecylmethylammonium picrate (**3**)

determined from the peak area of the DSC thermogram, while the transition entropy, ΔS (kJ mol^{-1} K^{-1}), was calculated by the equation $\Delta S = \Delta H/T$. All results were taken only from the first heating and cooling run as mean values of several independent measurements carried out on different samples of the same compound (Table 1).

High temperature WAXS measurements were made on a theta–theta diffractometer Ultima III, Rigaku, Japan) with oven sample chamber and scintillation counter as the detector. Step size was 0.02° and scan rate was 0.5° per minute. Data were analyzed in Jade 9 (MDI, Inc., CA). Detection was with a home made linear position sensitive detector.

Crystals of compounds suitable for single-crystal X-ray analysis were grown from acetone solutions by slow evaporation at −4 °C in refrigerator. All measurements were performed on Xcalibur Nova X-ray diffractometer with multilayer optics and Cu K_α radiation ($\lambda = 1.5412$ Å) at room temperature. Data reduction was performed using CrySalisPro software [15] and WINGX [16] program package. Structures were solved by direct methods using the SHELXS package and refined by SHELXL97 [17]. Molecular geometry calculations were done by PLATON98 [18]. Plots of the molecules and crystal packings were generated by MERCURY [19]. Atomic scattering factors were included in SHELXL97 and the hydrogen atom coordinates were geometrically calculated and refined using riding model of the same package. Crystallographic data for the structures **1**, **2**, and **3** are deposited in the Cambridge Structural Database under the CCDC codes 807677, 807678, and 807679, respectively.

Results and discussions

The general structural formulae of the investigated picrates are listed in Scheme 1. The compounds **1**–**3** are molecular addition salts of different cationic single-, double-, and three-tailed alkylammonium surfactants with picrate anion. Compounds differ in the number of dodecyl chains sited on the same nitrogen atom in quaternary ammonium groups. The structures and physico-chemical properties of selected molecules would yield new informations that are necessary for knowing the role of surfactant tails in controlling the shape and size of the resulting aggregates in solution and solid state.

Synthesis of cationic surfactant–picrate compounds

Synthesis of novel crystalline 1:1 ion-pair complexes (**1**–**3**) is based on electrostatic interactions between negatively charged phenolic oxygen from picrate counterion [3, 4], and postively charged nitrogen from surfactant headgroup. The formation of single- or multi-tailed surfactant–picrate

Table 1 The diameters for vesicles populations formed 2 and 14 h after preparation (t_A) and the period of vesicles stability (t_V) for the compounds **1** and **2**

Compound	t_A = 2 h (d/nm)		t_A = 14 h (d/μm)		t_V/days
1	560	8,500	8	35	1.0
2	35,000		2	5	2.6

compounds by spontaneous batch experiment in polar solvent can be described with Eq. 1:

$$\left[N^{+}(CH_3)_{4-x}R_x\right]X^{-} + H^{+}P^{-} \rightarrow \left[N^{+}(CH_3)_{4-x}R_x\right]P^{-} + H^{+} + X^{-}, \quad (1)$$

where R denotes dodecyl chain, P denotes picrate anion, x is the number of dodecyl chains, and X denotes halide counterions.

The synthesis of tetramethylammonium, tetraethylammonium [20], and tetrabutylammonium picrate was successfully carried out [21], but our attempted preparation of the tetradodecylammonium picrate complex in different media was unsuccessful, similar to the synthesis of tetraalkylammonium halide–catechol complexes [22]. Unlike complexes with shorter tetraalkyl chains, packing requirement of tetrabutylammonium cation points to energetically unfavorable bonding geometry [22].

Although this article is focused on thermal and structural properties of the solid surfactant picrates, some interesting macroscopic observations in bulk aqueous solutions during compounds preparation cannot be omitted. Immediately after mixing components all aqueous systems became multi-phased, characterized by the presence of spherical vesicles, or coexistence of precipitate and fused or desintegrated vesicles (Fig. 1). The presence of vesicles as time dependent and unstable discrete aggregates of bilayered structure with broad size distribution, indicates that precipitation proceeds via liquid crystalline phase formation.

In general, surfactant molecules self-assemble in water solutions into a large variety of morphologically different structures, depending on concentration and conditions in the bulk, molecular architecture, intermolecular interactions, addition of other surfactants or cosolutes, or application of external forces. Some of the promoters of bilayers and vesicles formation are electrostatic attractions and intermolecular hydrogen bonds. For ionic surfactant systems, the long range electrostatic forces play a dominant role in the aggregate structure and stability. Simple single-chained surfactant molecules rarely form vesicles if not mixed with negatively charged surfactants, or by salt addition. The addition of picrate counterion to investigated surfactant aqueous solutions containing unimers or micelles induces spontaneous formation of vesicles. These vesicles are metastable aggregates formed without external energy input (assuming a necessary shear during sample mixing as equal for all the samples), and demonstrate differently long transformation times. The compound **3** was prepared in acetone, no vesicels were observed in this medium and is not shown in Fig. 1 and Table 1. During the preparation of compound **2** with double-chained, didodecyldimethylammonium bromide surfactant, multilamellar vesicles were already present before mixing with picrate solution (size of about 50 μm, which is in good agreement with the data described earlier [13]). Addition of picrate counterion induces the transformation of vesicles and appearance of lamellar sheet fragments. As determined by optical microscopy, decreased size of 2 and 14 h aged vesicles (from initially 50, to 35 μm and 2 to 5 μm, respectively) points to vesicles breakdown. It seems that after the initial vesicle formation, the incorporation of picrates into vesicle structure of didodecyldimethylammonium bromide occurs, and then the subsequent disintegration of the vesicles, leading to further precipitation. Such a fusogenic behavior of didodecyldimethylammonium bilayer vesicles was demonstrated previously in the presence of variety of inorganic and organic anions [23]. The changes of vesicle size with aging time, t_A, is summarized in Table 1. Two populations of vesicles, significantly differing in size, were detected in the nanometer range (determined by DLS) 2 h after preparation of compound **1**. Changes in microelectrophoretic mobility were statisticaly distributed around zero charge, as expected. About 14 h after preparation, the size of vesicles in both populations increased to micrometer range (observed by optical microscope) and such vesicles are characterized as giant vesicles. Further change of giant vesicle size toward smaller values is accompanied with precipitate formation. Table 1 shows also the vesicles stability period, t_V, defined as the time in days during which one can still detect the vesicles, i.e. the time needed for complete transformation of vesicles. This transformation includes the transition of liquid crystalline phase to solid crystalline phase. It can be clearly seen that the number of dodecyl chains strongly influenced the t_V value. The stability period of liquid

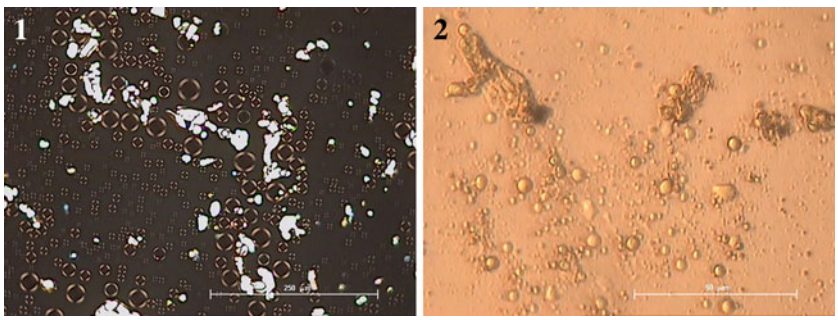

Fig. 1 The vesicles observed upon preparation the samples **1** and **2** under crossed polarizers (**1**) and using phase contrast (**2**). The microphotographs are taken 14 h after preparation of the systems at concentrations of about 5 mmol dm^{-3}. The bar corresponds to 250 μm

crystalline phase grew up with increased number of dodecyl chains bounded to the same headgroup (compounds **1** and **2**).

Microscopic observations (Fig. 1) and DLS measurements (Table 1) indicated that mechanism of liquid crystalline to solid crystalline phase transitions involves at least three steps: initially, the addition of oppositely charged picrates induces spontaneous formation of vesicles, further incorporation of picrates into vesicle structure induces growth of vesicles, and during prolonged aging breakdown of giant vesicular assemblies leads to the increasing amount of precipitate. Such transformations from vesicular, lyotropic systems, to the complex crystalline assemblies are governed by the headgroup electrostatic interactions of cationic surfactants with picrate counterion, respecting the different geometries of investigated surfactant molecules as well as picrate geometry.

The crystal structures

The crystal structures of many picrates have been determined with high precision, often used for comparison of the dimensions and conformations of the picrate ions in different crystallographic environments. The crystalline structure of dodecylammonium picrate belongs to triclinic symmetry, and the dodecyl chains in zig-zag conformation with the polar amino ends are packed in head-to-head orientation [3]. To establish the structure and packing arrangement of solid picrates, X-ray single-crystal analysis was used (Figs. 2, 3, 4). The single-tailed compound **1** crystallized in triclinic *P*-1 space group with two dodecylammonium and two picrate ions in the asymmetric unit. In the crystal packing, clear division of hydrophobic and hydrophilic layers is visible (Fig. 2). The picrate groups are stacked one on top of the other utilizing $\pi\ldots\pi$ stacking interactions with closest distance between C atoms of 3.29 Å. Each of the picrate groups forms C–H…O hydrogen bonds between their nitro groups and methyl groups of the dodecyltrimethylammonium cations. The distance between C and O atoms in these hydrogen bonds ranges from 3.08 to 3.18 Å. Long aliphatic tails of the dodecylammonium groups are placed next to each other thus forming a hydrophobic layer. The whole crystal packing is formed by the interchange of hydrophobic and hydrophilic layers. The introduction of three methyl groups on the N atom of alkyl chain in the compound **1** greatly reduces its hydrogen bond capability. This leads to the somewhat different crystal packings of the two compounds. In the case of dodecylammonium picrate [3], the polar head of alkyl chains is fully involved in bifurcated N–H...O hydrogen bonds with neighboring picrate anions which act as the bridges between them. In the crystal packing of **1**, the C–H…O hydrogen bonds are much weaker, and the packing is dominated by hydrophobic interactions between alkyl molecules and $\pi\ldots\pi$ interactions of the picrate aromatic rings. Each of the picrate groups forms C–H…O hydrogen bonds between their nitro groups and methyl groups of the dodecyltrimethylammonium cations. This lack of hydrogen bond ability may contribute to the doubling of the number of independent molecules in the asymmetric unit in the crystal structure of **1**. One of the dodecyltrimethylammonium molecules is slightly bent at the ammonium end of the molecule to accommodate the crystal packing.

In the crystal packing of double-tailed compound **2** (also space group *P*-1), the separation of hydrophobic and hydrophilic layers is even more pronounced than in the crystal packing of compound **1** (Fig. 3). The underlying network of noncovalent bonds and packing pattern are similar to the compound **1**. Picrate groups stack via $\pi\ldots\pi$ interactions (the closest C–C distance is 3.42 Å) and connect to the didodecyldimethylammonium cations with C–H…O hydrogen bonds.

The three-tailed compound **3** crystallizes in the space group *C* 2/c (Fig. 4). Two picrate molecules are

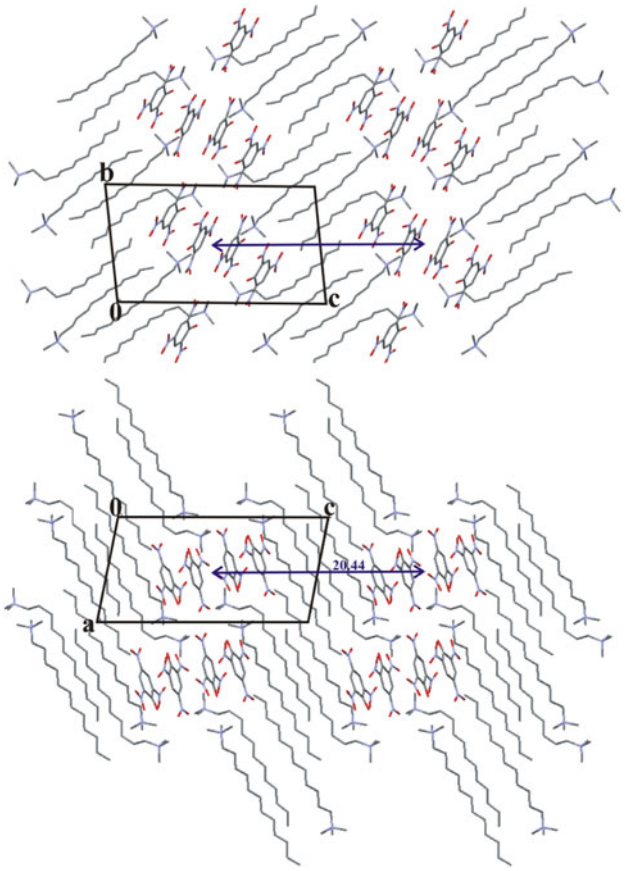

Fig. 2 Two views of the crystal packing of the compound **1**. The width of the layers is equal to the crystallographic *c* axis which is 20.44 Å

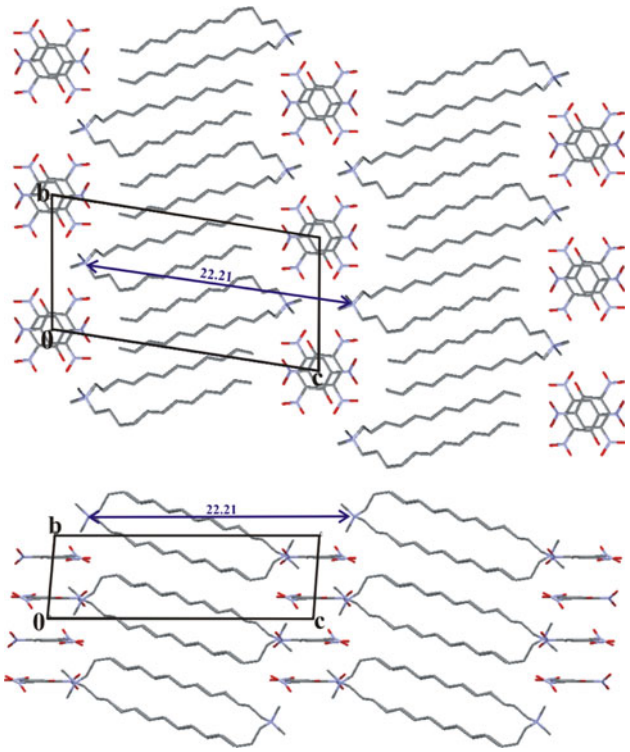

Fig. 3 The width of the layers in the structure **2** is equal to the crystallographic *c* axis which is 22.21 Å

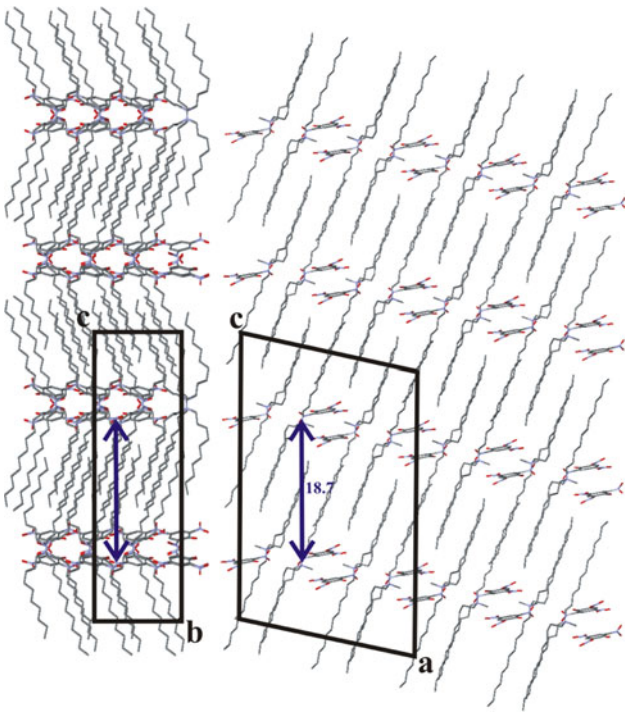

Fig. 4 Two views of the crystal packing of the compound **3.** The width of the layers is equal to the half of the crystallographic *c* axis which is 18.7 Å

"sandwiched" between three-tailed alkyl molecules and isolated from other molecules but form large number of C–H…O hydrogen bonds. The conformation of three-tailed alkylammonium cations is such that two long tails point in the opposite direction from the third tail. Molecules assemble in such a way that their long tails are placed in parallel to form one hydrophobic layer. Each picrate forms $\pi\ldots\pi$ interactions with only one neighboring picrate molecule (closest distance between C atoms in the aromatic rings is 3.34 Å). All of the oxygen atoms are involved as acceptors of C–H…O hydrogen bonds from the surrounding alkyl chains.

Crystallographic data, structure solution, and refinement for the compounds dodecyltrimethylammonium picrate (**1**), didodecyldimethylammonium (**2**), and tridodecylmethylammonium picrate (**3**) are given in Table 2.

The stacked bilayered structures are characteristic for the behavior of amphiphilic compounds with *n*-alkyl chains [24]. The similarity of the synthetic surfactant molecular assembly with bilayer strucuture to those of phospholipids is evident [25], but also their ability to conform desired bilayer assemblies in the form of single crystal [25]. The intralamellar electrostatic interactions between cationic and anionic fragments neutralize the surface charge through the formation of tight ion pairs, and alternatively accomodation of hydrophilic and hydrophobic regions is well known [24]. The investigated series of aggregation structures formed spontaneously in single crystals (**1**–**3**) of amphiphile-picrate compounds shows bilayer forming properties, similar to that of bilayers in biomembranes. Crystal packing of these compounds (Figs. 2, 3 and 4) does not point to the classical bilayer, but to the distinctive bilayers formation interrupted with layers of polar heads and picrate counterions. Unique properties of this crystal structures are based on molecular ordering with typical width of such a bilayers equal to the crystallographic *c* axis which is 20.44 Å (**1**) and 22.21 Å (**2**); or equal to the half of *c* axis for compound **3** which is 18.7 Å. The crystals of dodecyltrimethylammonium bromide (DTAB) have a smectic layer structures stacked along the *c* axis, and show tail to head packing [24], i.e. chains lay parallel to one another and head groups are oriented in opposite direction. The insertion of picrate molecule to form compound **1** ($c = 20.44$ Å, Fig. 2) does not cause the elongation of *c* axis length in comparison with DTAB crystal itself ($c = 21.55$ Å) [24]. Independent of temperature, for didodecyldimethylammonium bromide the lattice parameter $a = 6.04$, the width of layers of 23.6 Å, and also an ordered two dimensional tetragonal arrangement of the ionic ammonium bromide groups within the smectic layers [26] was determined. However, when picrate instead of bromide acts as counterion, the picrate compound **2** shows elongation of parameter *a* to 6.95 Å, and low compression

Table 2 Crystallographic data, structure solution, and refinement for the compounds **1–3**

Identification code	1	2	3
Empirical formula	$C_{42}H_{72}N_8O_{14}$	$C_{32}H_{58}N_4O_7$	$C_{43}H_{80}N_4O_7$
Formula weight	913.08	610.82	765.11
Temperature/°K	293(2)	293(2)	293(2)
Wavelength	1.5418 Å	1.5418 Å	1.5418 Å
Crystal system	Triclinic	Triclinic	Monoclinic
Space group	*P*-1	*P*-1	*C* 2/c
Unit cell dimensions/Å, °	$a = 11.1136(5)$	$a = 6.9546(8)$	$a = 23.5896(10)$
	$b = 12.1995(5)$	$b = 11.0626(8)$	$b = 11.0371(3)$
	$c = 20.4439(10)$	$c = 22.210(2)$	$c = 37.4593(15)$
	$\alpha = 92.433(4)$	$\alpha = 98.423(7)$	$\beta = 101.546(4)$
	$\beta = 99.601(4)$	$\beta = 93.735(8)$	
	$\gamma = 111.112(4)$	$\gamma = 96.066(7)$	
Volume/Å^3	2533.6(2)	1675.2(3)	9555.6(6)
Z	2	2	8
Density (calculated)/mg/m^3	1.197	1.211	1.064
Absorption coefficient/mm^{-1}	0.747	0.685	0.564
F(000)	984	668	3376
Crystal size/mm	0.1 × 0.1 × 0.2	0.1 × 0.1 × 0.1	0.3 × 0.2 × 0.2
Theta range for data collection/°	3.91–54.21	4.07–62.26	4.09–58.93
Index ranges	$-11 \le h \le 11$,	$-7 \le h \le 6$,	$-26 \le h \le 24$,
	$-12 \le k \le 11$,	$-12 \le k \le 8$,	$-12 \le k \le 11$,
	$-21 \le l \le 21$	$-24 \le l \le 25$	$-41 \le l \le 41$
Reflections collected	18842	10416	20313
Independent reflections	6160 [*R*(int) = 0.0348]	5126 [*R*(int) = 0.0577]	6831 [*R*(int) = 0.0414]
Completeness/%	99.5	96.9	99.3
Refinement method	Full-matrix least-squares on F^2	Full-matrix least-squares on F^2	Full-matrix least-squares on F^2
Data/restraints/parameters	6160/0/578	5126/0/388	6831/0/469
Goodness-of-fit on F^2	1.219	1.094	1.822
Final *R* indices [$I > 2$sigma (I)]	$R_1 = 0.0967$	$R_1 = 0.0701$	$R_1 = 0.1391$
	$wR_2 = 0.2946$	$wR_2 = 0.1959$	$wR_2 = 0.4142$
R indices (all data)	$R_1 = 0.1232$	$R_1 = 0.1058$	$R_1 = 0.1530$
	$wR_2 = 0.3229$	$wR_2 = 0.2193$	$wR_2 = 0.4282$
Largest diff. peak and hole/e/Å^3	0.510 and −0.314	0.352 and −0.361	1.522 and −0.344

of layers width to 22.21 Å. The crystal structure of dioctadecyldimethylammonium bromide consists also of bimolecular layers with characteristic tail to tail packing [25], while the investigated didodecyldimethylammonium picrate shows alternate head to tail layout (Fig. 3). The crystal packing of compound **3** cannot be compared to the crystal structure of tridodecylmethylammonium chloride surfactant itself because this structure is not solved. Two picrate molecules of compound **3** are "sandwhiched" between three-tailed alkyl molecules and isolated from other molecules but form large number of C–H…O hydrogen bond (Fig. 4).

Consequently, the analysis of this structures strongly suggests that theirs solids are partly like synthetic bilayers and consist of repeated patterns characteristic for liquid crystalline phases interrupted with layers of polar heads and picrate counterions. The observed widths of bilayers of the investigated picrates **1–3** (Figs. 2, 3, 4) are not simple functions of the number of dodecyl chains on the same nitrogen atom in quaternary ammonium groups, but are the consequences of more complex structural behaviors which ensures alternation in space of equal numbers of positive and negative charges, as required by thermodynamics for systems with electrostatic interactions.

Thermal properties

The crystals most of alkylammonium amphiphiles exhibit numerous quantitative variations of the bilayer structures with complex polymorphism and mesomorphism, as a

function of temperature [11]. Diferent alkyltrimethylammonium halides undergo the processes of solid–solid phase transition to melting of the alkyl chains, without formation of liquid crystalline phase [27]. Bromides are thermally unstable and decompose before melting [28]. Dialkyldimethylammonium bromides show thermotropic mesomorphism with marked hysteresis upon cooling and a complex polymorphism of the crystalline state, with a variety of coexisting metastable crystal forms, when reached by cooling from the melt [26]. The smectic mesophase of didodecyldimethylammonium bromide is characterized between 344 and 441 K in heating cycle, and down to the 317 K in cooling cycle [26]. The thermal and mesogenic properties of muli-tailed surfactants are poorly described, mostly whiting the meaning of polyfunctional derivatives or carcinostatic and antibacterial drugs. Due to the lack of trialkylmethylammonium halide data, the thermal analysis of the single component tridodecylmethylammonium chloride (TDMAC) as three-tailed component was carried out first. The component passes through reproducible exothermic transitions during cooling, and endothermic transitions during heating. The phase transition parameters, transition temperatures, and enthalpy changes derived form DSC heating and cooling scans are listed in Table 3. The thermogram of TDMAC is shown in Fig. 5 and micrographs of the characteristic textures formed by heating and cooling of the sample in Fig. 6. Component TDMAC is solid crystal at room temperature (not shown) and at characteristic elevated temperature it exhibits properties of liquid crystal (LC). Furthermore, as it can be seen in Table 4, the TDMAC sample analyzed by

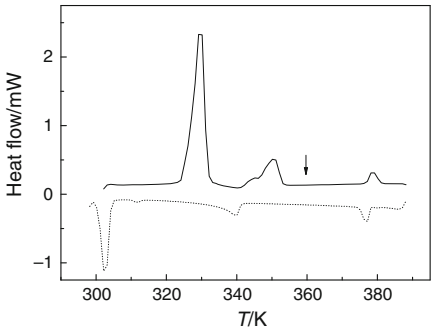

Fig. 5 The thermogram of tridodecylmethylammonium chloride (TDMAC) obtained by differential scanning calorimetry during heating (endothermic transitions, *full lines*), and cooling runs (exothermic transitions, *dashed lines*). The *arrow* indicates the temperature of WAXS measurement

XRD at 358 K displays sharp peaks with reciprocal spacings in the ratio 1:2:3:5 and is indexed as lamellar LC. There is a diffuse peak in the diffraction pattern in the vicinity of 4.5 Å which is characteristic of flexible and molten state of hydrocarbon chains.

Polarizing microscopy studies of the textures (Fig. 6) formed upon heating and cooling the isotropic melt to room temperature of TDMAC confirmed the identified mesophases and characterized sample as enantiotropic. The TDMAC images shown in Fig. 6a display spherulites–maltese crosses and typical "oily streaks", and Fig. 6b displays stepped drop texture (phase contrast), all of them significant for lamellar phase. The low enthalpy changes values for mesomorphic to isotropic liquid transition and vice versa (Table 3) are also indications for respective

Table 3 Transition temperatures, T/K, enthalpies, ΔH/kJ mol^{-1}; and entropies, ΔS/J mol^{-1} K^{-1}, of tridodecylmethylammonium chloride (TDMAC)

Compound	Heating			Cooling		
	T/K	ΔH/kJ mol^{-1}	ΔS/J mol^{-1} K^{-1}	T/K	ΔH/kJ mol^{-1}	ΔS/J mol^{-1} K^{-1}
TDMAC	323	59.1	179.4	377	−3.3	−8.6
	351	15.6	44.6	340	−6.5	−19.2
	379	2.9	7.7	312	−0.5	−1.7
				303	−17.5	−57.9

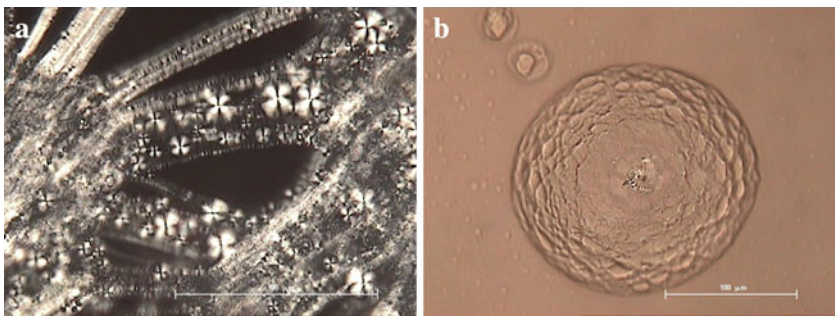

Fig. 6 The micrographs of the characteristic textures formed by heating (**a**) and cooling to room temperature (**b**) of TDMAC, as observed on the microscope hot stage by crossed polarizers (**a**) and phase contrast (**b**). T/K = 353 K (**a**) and 298 K (**b**). The bar represents 100 μm (**a**) and 50 μm (**b**)

Table 4 Interplanar spacings, d, Miller indices, 00l, and relative intensities, I_{rel}, for tridodecylmethylammonium chloride (TDMAC) at 358 K

TDMAC, $T = 358$ K		
d/Å	00l	I_{rel}
23.5	001	100
12.0	002	56
7.9	003	42
4.6	005	7

mesomorphic transformations**.** Moreover, other transitions detected at lower temperatures during heating originate most probaly from solid-state polymorphism, which corresponds to the gradual increasing disorder of the alkyl chains upon heating. Picric acid and their salt with dodecyl-chain amine [3] do not show thermotropic properties.

The thermal stabilities of investigated picrates were analyzed systematically by thermogravimetry. They are found not to decompose below 445 K. Table 5 summarizes phase transition parameters, individual transition temperatures, and changes in enthalpy and entropy of compounds **1**–**3**, derived from the DSC heating and cooling scans, in comparison with dodecylammonium picrate (DAP) [3]. Microscopically obtained changes that occured at specific temperatures were in aggreement with the DSC measuremets.

It can be seen on the thermogram of dodecyltrimethylammonium picrate (compound **1**), that the same number of endothermic transitions during heating and exothermic transitions during cooling cycle occured, corresponding to the two different transitions in the solid crystalline state. The only difference between compounds DAP and **1** is the presence of three methyl groups on the amino group in **1** instead of hydrogens in DAP, and obviously different molecular conformations and associated conformational disorders are responsible for differences in the packing and properties of solid–solid polymorphs [29]. Moreover, the methyl groups can exert a greater steric strain because of their greater electron density compared to hydrogen. The thermal hysteresis of the phase transition temperatures for melting to crystallization processes ($\Delta T = T_M - T_C$) is observed. By the introduction of three methyl groups (comparison of compounds DAP and **1**), the difference of the melting and crystallization temperatures decreases ten times ($\Delta T_{DAP} \sim 51$ K [3] and $\Delta T_{\mathbf{1}} \sim 5$ K). The phenomenon of thermal hysteresis is associated to the presence of metastable states and is characteristic of the first order phase transition.

Compounds **2** and **3** showed markedly slugged crystallization from the melt and it took time in hours (**2**) and days (**3**) for crystals to develop, as monitored microscopically. Figure 7 shows representative DSC curves of compounds **1** and **2** during heating and cooling runs (upper part), and the zig-zag blade crystalline textures (lower part) of **1** (a), **2** developed 36 h (b), and **3** developed 54 h (c) after melting and cooling to room temperature.

For all of the investigated picrates, there are no indications of the thermotropic mesomorphism, as was also found for dodecylammonium picrate [3]. The absence of mesomorphic properties can be attributed to the dominant effect of picrate molecules with favorable interlayer 3-D hydrogen bond network between amino and picrate groups. The ionic layer, formed of amino and picrate groups, is "sandwiched" between the hydrocarbon chain layers, which cause alienation of hydrocarbon bilayers. As the Coulomb interactions are stronger compared to van der Waals forces in the hydrocarbon layers, one would expect the ionic layers to remain unchanged by heating, with conformational or positional disorder at lower temperatures, possessing the liquid crystalline properties. Usually, this disorder of ionic layers causes changes at higher temperatures, from the liquid crystalline phase to the isotropic liquid disorder. Unlike this, the existence of well-defined melting points, as mostly only phase transition in examined picrates, indicates the fact that disordering of dodecyl chains and the destruction of ionic layers occures simultaneously during melting of picrates, their liquid

Table 5 Transition temperatures T/K, enthalpies ΔH/kJ mol^{-1}, and entropies ΔS/J mol^{-1} K^{-1} of investigated picrate compounds **1**–**3**, in comparison with dodecylammonium picrate (DAP) [3]

Compound	Heating			Cooling		
	T/K	ΔH/kJ mol^{-1}	ΔS/J mol^{-1} K^{-1}	T/K	ΔH/kJ mol^{-1}	ΔS/J mol^{-1} K^{-1}
DAP [3]	386	39.2	101.6	335	−34.3	−102.3
1	325	14.9	45.8	310	−3.5	−11.1
	341	2.8	8.2	336	−2.9	−8.7
	386	16.0	41.5	381	−16.1	−42.2
2	314	71.3	226.9	No detectable changes		
3	331	83.3	251.7	No detectable changes		

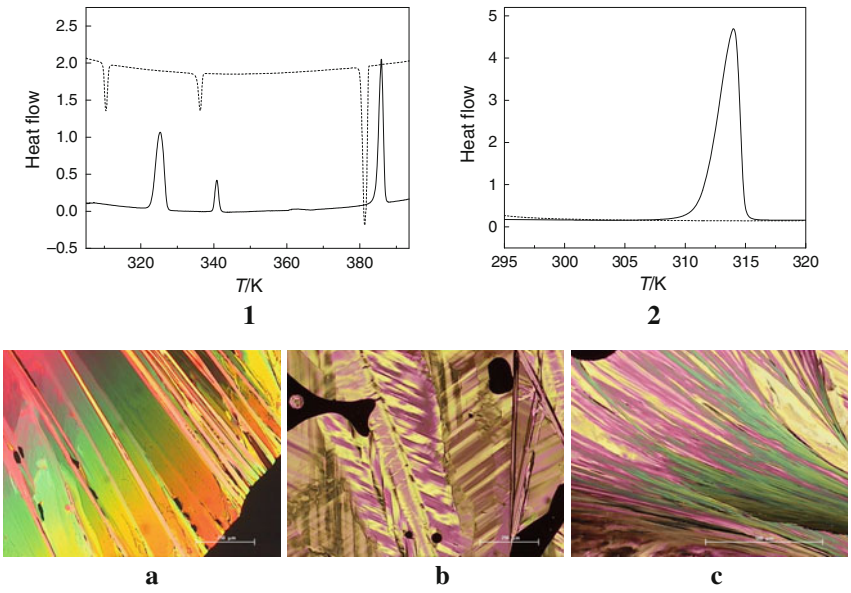

Fig. 7 *Upper part*: the thermogram of dodecyltrimethylammonium picrate (**1**), and didodecyldimethylammonium picrate (**2**), obtained by DSC during heating (endothermic transitions, *full lines*), and cooling runs (exothermic transitions, *dashed lines*). *Lower part*: cross-polarized microscopy images of **1** (**a**), **2** developed 36 h (**b**), and **3** developed 54 h after melting and cooling to room temperature (**c**). The bar represents 250 μm (**a**, **b**) and 500 μm (**c**)

crystalline properties are not pronounced and they cannot be characterized as thermotropic compounds. Difficult and slugged crystallization from the disordered to the ordered phase of the samples from the melt, points the uncommon ordering and kinetically managed processes. In addition, the architecture of cationic surfactants with increased dodecyl chain number makes this process more complicated and also slower. This is the good reason for the importance of examinations of the structural arrangements composed of ionic and lipid layers with components of different dimensions, architectures, and their hydrophilic–hydrophobic nature.

Considering the thermodynamic parameters of investigated picrates (Table 5, Fig. 8) by varying the number of dodecyl chains (n_D = 1–3) for compounds **1** (n_D = 1), **2** (n_D = 2), and **3** (n_D = 3), overall melting enthalpies (dH_M) and entropies (dS_M) follow linear growth by the Eqs. 2 (R = 0.96) and 3 (R = 0.93):

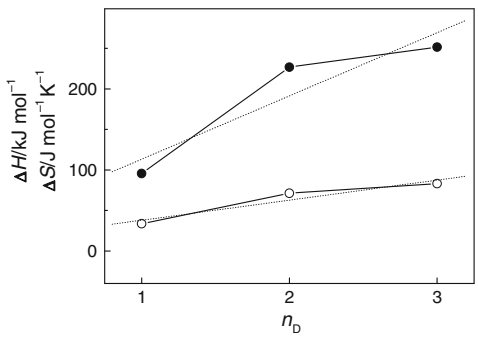

Fig. 8 The dependence of transition enthalpies (ΔH/kJ mol^{-1}, *open circle*) and entropies (ΔS/J mol^{-1} K^{-1}, *solid circle*) versus the number of dodecyl chains sited on the same amino group (n_D) of investigated picrates in heating cycle

$$dH_M/\text{kJ mol}^{-1} = 24.8n_D + 13.2 \quad (2)$$

and

$$dS_M/\text{J mol}^{-1}\text{K}^{-1} = 78.1n_D + 35.3. \quad (3)$$

Many published data of surfactant-based compounds found the explicit proportionallity of increasing hydrocarbon chain length, and different physico-chemical transitions, theirs entropy changes and temperatures at which they occur. The dependence on the number of dodecyl chains sited on the same nitrogen atom in quaternary ammonium group of the samples **1**–**3** was not found for melting temperatures, but for melting enthalpies and entropies. The increase of melting entropies indicates an enhanced disorder by increasing n_D, which is in accordance with layout of more complexed structures.

It is interesting to see how the variation of chain number affects the transitions and physico-chemical properties of other picrate–surfactant derivatives. To get better insight into the structure–properties relationship, our work on the impact of the alkyl chain number in oligomeric surfactants is in progress.

Conclusions

The crystalline materials of three novel surfactant–picrate compounds were synthesized and characterized through elemental analysis, thermogravimetric, thermal transitions analysis, optical polarizing microscope, and by single-crystal XRD techniques.

The picric acid acts as promoter of lyotropic properties in reaction with oppositely charged single- and multi-tailed dodecylammonium cationic surfactants. The analysis of crystallographic structures suggests that theirs solids are partly like paraffin-like bilayers, consisted of alternated hydrophobic and hydrophilic layers. Regular selfassembled hydrophobic alkyl chains are interrupted with layers of polar heads and picrate counterions. Parallel with the growing complexity of cationic part of picrate crystals the separation of the hydrophobic and hydrophilic domains is less pronounced. The variations of the observed width of the bilayers are not functions of the number of dodecyl chains, but are the consequences of more complex mutual packing behaviors which ensures alternation in space of equal numbers of positive and negative charges, as required by thermodynamics for systems with electrostatic interactions. Unlike dodecyltrimethylammonium bromide and picric acid, didodecyldimethylammonium bromide and tridodecylmethylammonium chloride solid crystals possess smectic properties. No thermotropic properties of investigated picrate compounds are detected which can be attributed to the dominant effect of picrate molecules with favorable interlayer 3-D hydrogen bond network between amino and picrate groups.

The increase of the thermodynamic parameters in heating cycle depends linear on the number of alkyl chains. The pronounced kinetic hindering of solidification for multi-tailed picrate molecules was observed, and this period is longer for more complex strucutures.

Acknowledgements This work was supported by the Ministry of the Science, Education, and Sport of the Republic of Croatia (Project Nos 098-0982915-2949 and 098-1191344-2943). We are grateful to Dr. Ellen Wachtel, Department of Materials and Interfaces, Weizmann Institute of Science, Israel, for carrying out the XRD experiments.

References

1. Olsher U, Feinberg H, Frollow F, Shoham G. The picrate anion as a versatile chelating counter-ion for the complexation of alkali and alkaline earth metal cations with ionophores: "The picrate effect". Pure Appl Chem. 1996;68:1195–9.
2. Farrell PG, Shahidi F, Casellato F, Vecchi C, Girelli A. DSC studies of aromatic hydrocarbon picrates. Thermochim Acta. 1979;33:275–80.
3. Tomašić V, Tušek-Božić LJ, Višnjevac A, Kojić-Prodić B, Filipović-Vinceković N. Physicochemical properties of dodecylammonium picrate. J Colloid Interface Sci. 2000;227:427–36.
4. Ohba S, Ito Y. 2-(4-Hydroxyphenyl)ethylammonium picrate. Acta Cryst E. 2002;58:584–5.
5. Martin Britto Dhas SA, Natarajan S. Growth and characterization of a new potential second harmonic generation material from the amino acid family: L-Valinium picrate. Cryst Res Technol. 2008;43:869–73.
6. Goto M, Kanno H, Sugaya E, Osa Y, Takayanagi H. Crystal structure of adenosinium picrate. Anal Sci. 2004;20:39–40.
7. Anitha K, Athimoolam S, Natarajan S. Pyridoxinium picrate. Acta Cryst C. 2006;62:426–8.
8. Marchand AP, Hazlewood A, Huang Z, Vadlakonda SK, Rocha JDR, Power TD, et al. Stabilization of a K+-(bis cage annulated 20-crown-6) complex by bidentate picrate. Struct Chem. 2003; 14:279–88.
9. Nagarajan R. Molecular packing parameter and surfactant self-assembly: the neglected role of the surfactant tail. Langmuir. 2002;18:31–8.
10. Ungar G, Tomašić V, Xie F, Zeng X-b. Structure of liquid crystalline aerosol-OT and its alkylammonium salts. Langmuir. 2009;25:11067–72.
11. Terreros A, Galera-Gomez PA, Lopez-Cabaracos E. DSC and X-ray diffraction study of polymorphism in n-alkylammonium chlorides. J Therm Anal Calorim. 2000;61:341–50.
12. Esson JM, Ramamurthy N, Meyerhoff ME. Polyelectrolyte-surfactant complexes: an aqueous titration method to model ion-pairing within polymeric membranes of polyion-sensitive electrodes. Anal Chim Acta. 2000;404:83–94.
13. Ono Y, Kawasaki H, Annaka M, Maeda H. Effects of micelle-to-vesicle transitions on the degree of counterion binding. J Colloid Interface Sci. 2005;287:685–93.
14. Marques EF, Regev O, Khan A, da Graca Miguel M, Lindman B. Vesicle formation and general phase behavior in the catanionic mixture SDS–DDAB–water. The cationicrich side. J Phys Chem B. 1999;103:8353–63.
15. Harms K, Wolcado S. XCAD4-CAD4 data reduction. Germany: Universitiy of Marburg; 1995.
16. Farrugia LJ, Win GX. Suite for single crystal small molecule crystallography. J Appl Cryst. 1999;32:837–8.
17. Sheldrick GM. SHELX97: program for the refinement of the crystal structures. Germany: Universitiy of Gottingen; 1997.
18. Spek AL. PLATON 98: a multipurpose crystallographic tool 101201 version. Utrecht, The Netherlands: University of Utrecht; 2001.
19. Macrae CF, Edgington PR, McCabe P, Pidcock E, Shields GP, Taylor R, et al. Mercury: visualization and analysis of crystal structures. J Appl Cryst. 2006;39:453–7.
20. Finch A, Smith AE. Thermochemistry of picrates. III. Enthalpies of solution and solubities of picrate salts. Thermochim Acta. 1982;53:349–56.
21. Everaert J, Persoons A. Dissociation mechanism of tetrabutylammonium picrate ion pairs in media of low polarity. 1. A sphere-in-continuum approach. J Phys Chem. 1981;85:3930–7.
22. Khan MA. Hydrogen bonding and crystal packing trends in tetraalkylammonium halide-catechol complexes: synthesis, spectroscopic and crystal structure studies of Me4NC1-catechol, Et4NCl-catechol, Et4NBr-catechol and Pr4NBr-catechol complexes. J Mol Struct. 1986;145:203–18.
23. Rupert LAM, Hoekstra D, Engberts JBFN. Fusogenic behavior of didodecyldimethylammonium bromide bilayer vesicles. J Am Chem Soc. 1985;107:2628–31.
24. Kamitori S, Sumimoto V, Vongbupnimit K, Noguchi K, Okuyama K. Molecular and crystal-structures of dodecyltrimethylammonium bromide and its complex with P-Phenylphenol. Mol Cryst Liq Cryst. 1997;300:31–43.
25. Okuyana K, Soboi Y, Ijima N, Hirabayashi K, Kunitake T, Kajiyama T. Molecular and crystal structure of the lipid-model amphiphile, dioctadecyldimethylammonium bromide monohydrate. Bull Chem Soc Jpn. 1988;61:1485–90.
26. Alami E, Levy H, Zana R, Weber P, Skoulios A. A new smectic mesophase with two dimensional tetragonal symmetry from dialkyldimethylammonium bromides: ST. Liq Cryst. 1993;13: 201–12.

27. Iwamoto K, Ohnuki Y, Sawada K, Senō M. Solid-solid phase transitions of long-chain n-alkyltrimethylammonium halides. Mol Cryst Liq Cryst. 1981;73:95–103.
28. Malliaris A, Christias C, Margomenou-Leonidopoulou G, Paleos CM. Single chain quaternary ammonium salts exhibiting thermotropic mesomorphism and organization in water. Mol Cryst Liq Cryst. 1982;82:161–6.
29. Gilson DFR, Kertes AS, Manley RSJ, Tsau J, Donnay G. Polymorphism in n-alkylammonium chlorides: X-ray powder diffraction studies. Can J Chem. 1976;54:765–8.